Journal of Pharmaceutical and Biomedical Analysis 204 (2021) 114268

Contents lists available at ScienceDirect

Journal of Pharmaceutical and Biomedical Analysis

journal homepage: www.elsevier.com/locate/jpba

A label-free impedance biosensing assay based on CRISPR/Cas12a collateral activity for bacterial DNA detection

Andrea Bonini [a,*], Noemi Poma [a], Federico Vivaldi [a,b], Denise Biagini [a], Daria Bottai [c], Arianna Tavanti [c,**,1], Fabio Di Francesco [a,d,*,1]

[a] Department of Chemistry and Industrial Chemistry, University of Pisa, Via G. Moruzzi 13, Pisa, Italy
[b] Institute of Clinical Physiology, National Research Council, Via G. Moruzzi 1, Pisa, Italy
[c] Department of Biology, University of Pisa, Via San Zeno 35-39, Pisa, Italy
[d] INSTM, Via G. Giusti 9, Florence, Italy

ARTICLE INFO

Article history:
Received 10 March 2021
Received in revised form 10 July 2021
Accepted 12 July 2021
Available online 14 July 2021

Keywords:
Electrochemical CRISPR/Cas biosensing
Cas12a/gRNA
EIS
E. coli
S. aureus
Sepsis

ABSTRACT

The rapid and selective identification in the clinical setting of pathogenic bacteria causing healthcare associated infections (HAIs) and in particular blood stream infections (BSIs) is a major challenge, as the number of people affected worldwide and the associated mortality are on the rise. In fact, traditional laboratory techniques such culture and polymerase chain reaction (PCR)-based methodologies are often associated to long turnaround times, which justify the pressing need for the development of rapid, specific and portable point of care devices. The recently discovered clustered regularly interspaced short palindromic repeat loci (CRISPR) and the new class of programmable endonuclease enzymes called CRISPR associated proteins (Cas) have revolutionised molecular diagnostics. The use of Cas proteins in optical and electrochemical biosensing devices has significantly improved the detection of nucleic acids in clinical samples. In this study, a CRISPR/Cas12a system was coupled with electrochemical impedance spectroscopy (EIS) measurements to develop a label-free biosensing assay for the detection of *Escherichia coli* and *Staphylococcus aureus*, two bacterial species commonly associated to BSI infections. The programmable Cas12a endonuclease activity, induced by a specific guide RNA (gRNA), and the triggered collateral activity were assessed in *in vitro* restriction analyses, and evaluated thanks to impedance measurements using a modified gold electrode. The Cas12a/gRNA system was able to specifically recognize amplicons from different clinical isolates of *E. coli* and *S. aureus* with a limit of detection of 3 nM and a short turnaround time approximately of 1.5 h. To the best of our knowledge, this is the first biosensing device based on CRISPR/Cas12a label free impedance assay.

1. Introduction

The rapid detection of pathogenic agents involved in HAIs represents today one of the main challenges for an efficient disease control in the clinical setting. These infections, and in particular BSIs, are on the rise and cause a heavy burden of morbidity and mortality in internal medicine wards worldwide [1]. BSIs can result from surgery, the use of intravascular devices such as catheters or the migration of pathogens from other infected tissues or organs. Pathogens responsible for BSI include bacteria, viruses and fungi [2], but bacteria are the most common causative agents of disseminated infections (over 90 %) leading to sepsis. Sepsis is defined as "a life-threatening organ dysfunction caused by a dysregulated host response to infection", a condition that can result in the death of the patient if not promptly diagnosticated and adequately treated [3]. According to the World Health Organization, more than 30 million cases of sepsis are estimated to occur annually worldwide, with a mortality rate of 33–35 % and an incidence increasing 9–13 % annually [4]. Unfortunately, these numbers are destinated to increase with the exponential growth of hospitalized patients due to the actual COVID-19 pandemic and other comorbidities [5]. In addition, the rise of antibiotic resistance in clinically relevant bacteria

* Corresponding author at: Department of Chemistry and Industrial Chemistry, University of Pisa, Via G. Moruzzi 13, Pisa, Italy.
** Corresponding author at: Department of Biology, University of PIsa, Via San Zeno 35-39. Pisa, Italy.
E-mail addresses: andrea.bonini@phd.unipi.it (A. Bonini), n.pomasajama@studenti.unipi.it (N. Poma), federicomaria.vivaldi@phd.unipi.it (F. Vivaldi), denisebiagini@virgilio.it (D. Biagini), daria.bottai@unipi.it (D. Bottai), arianna.tavanti@unipi.it (A. Tavanti), fabio.difranceco@unipi.it (F. Di Francesco).
[1] These authors equally contributed to this work.

https://doi.org/10.1016/j.jpba.2021.114268
0731-7085/

is particularly alarming [6]. Conventional blood culture techniques, flanked by molecular techniques based PCR), are considered the reference method for the identification of pathogenic bacteria from BSIs [7]. However, blood culture is a time consuming procedure, and PCR-molecular approaches require trained personnel, dedicated instrumentation and expensive reagents [8]. Furthermore, due to the low concentration of bacteria in bloodstream infections, an amplification step is always required. Unfortunately, PCR methods are not easily implemented in portable biosensing devices. Despite the recent development of many alternative isothermal amplification methods such as loop-mediated isothermal amplification (LAMP), rolling circle amplification (RCA), strand displacement amplification (SDA), exponential amplification reaction (EXPAR) recombinase polymerase amplification (RPA) the situation has not been improved [9]. The detrimental impact on social and economic costs of congested laboratory routines for the detection of pathogenic agents dramatically spurs companies and scientific community to conceive new detection strategies to be implemented in portable devices allowing a rapid, specific and selective identification at the clinic. Biosensor devices and technology may play an important role in such innovation in the near future [10].

Several affinity biosensors for the detection of whole bacteria have been developed, but unfortunately these systems have limitations. Indeed, it display low selectivity and specificity against their bacterial target, providing such systems with low flexibility and making them useful only towards a limited number of bacteria [11]. These limitations make these systems not attractive for the routine detection of microorganisms involved in BSIs.

The recently discovered CRISPR/Cas system represented a major breakthrough in the portfolio of biorecognition elements useful to develop new nucleic acid biosensing strategies [12]. The CRISPR/Cas system is a nucleic acid based adaptive immune system against the viral infection discovered in Archaea and Bacteria [12]. The Cas proteins associated to the CRISPR *loci* are a family of programmable endonuclease enzymes (Cas9, dCas9, Cas13a, Cas12a), which are highly selective and specific when guided by a specific gRNA complementary to the recognition site on the target DNA/RNA [13]. The use of programmable Cas proteins in the development of optical biosensing devices has been demonstrated by several authors [12]. In these systems, the coupling of Cas proteins with isothermal amplification techniques has successfully overcome usual disadvantages of conventional amplification methods [12]. Recently, electrochemical biosensors based on Cas13a [14] and dCas9 [15] proteins were also developed, and in particular the Cas12a endonuclease activities against the target DNA encompassing a programmable activity (cis-activity) and an aspecific collateral activity (trans-activity) were investigated. In this respect, the Cas12a trans activity was recently validated using methylene blue tagged single strand DNA (MB-ssDNA) on a gold electrode surface [16]. This sensor, called E-CRISPR, exploited the Cas12/gRNA capability to specifically recognize the double strand DNA (dsDNA) of HPV-16 virus in solution, which triggers its collateral activity cutting the MB-ssDNA on the electrode surface. The E-CRISPR performance was subsequently improved using a methylene blue tagged hairpin DNA immobilized on gold electrode surface [17], while Xu and coworkers [18] demonstrated that the use of cis-activity to directly cleave the probe and the target dsDNA complex on the electrode surface was more effective than trans collateral activity in detecting the targeted Parvovirus B19 sequence.

In a scenario where most electrochemical biosensors employ a labelled MB-ssDNA on the electrode surface for the detection of an amplified target DNA, we propose an easy use, rapid and low cost detection system based on a label free ssDNA immobilized on a gold electrode. Our electrochemical impedance biosensor based on a Cas12a protein was tested for the detection of elected bacterial pathogens (*E. coli* and *S. aureus*) often associated to BSIs infections. EIS is a sensitive and powerful technique detecting subtle physical and chemical changes occurring at the electrode surface [19]. It can be easily implemented in low cost, portable, easy to miniaturize devices and has an inherent potential for label-free analysis. Due to these characteristics, impedance based devices have attracted lots of attention in the field of clinical diagnosis [20]. A recent study by Uygun [21] describes the development of an impedimetric biosensor for detection of circulating tumour DNAs using dCas9. Here, we report a new label-free biosensing assay based on the specific, and collateral activity of Cas12a endonuclease, thus expanding the use of the EIS technique to other enzymes of the Cas family.

2. Material and methods

2.1. Bacteria strains and growth conditions

Gram-negative (*Escherichia coli* ATCC25922) and Gram-positive (*Staphylococcus aureus* ATCC6538) reference laboratory strains were selected as model organisms to study the Cas12a/gRNA activities and in EIS based biosensor development. Reference strains were purchased from the American Type Culture Collection (ATCC, Manassas, Virginia, USA). Moreover, a panel of clinical isolates, selected from a collection of bacterial strains stored at the Department of Biology, Microbiology section, University of Pisa (see Table 1 supplementary information), was also used to evaluate the specific Cas12a/gRNA system activities.

All strains were stored at −80 °C in fresh Luria Bertani broth (LB, ThermoFisher Scientific, Waltham, Massachusetts, USA) supplemented with 30 % glycerol. Bacteria were growth on LB agar/broth (PanReac AppliChem GmbH, Darmstadt, Germany) at 37 °C for 18 h.

2.2. Gene selection and amplification

From each bacterial species a species-specific gene was selected and used as a target for Cas12a/gRNA system. The malate dehydrogenase (*mdh*, GenBank GeneID: 947854) and thermonuclease (*nuc*, GenBank GeneID: 45574557) encoding genes were selected for *E. coli* and *S. aureus,* respectively.

Internal primers were designed for each gene (see Table 2 supplementary information) and purchased in lyophilizate form (Merck KGaA, Darmstadt, Germany). Primers were resuspended in nuclease free water (100 μM solution) and diluted to 10 μM, then stored at −20 °C.

A bacterial pellet was boiled in sterile water for 1 min in order to achieve thermal lysis. 932 bp-*mdh* and 689 bp-*nuc* gene fragments were amplified from *E. coli* and *S. aureus* genomic DNA, respectively, using: DreamTaq DNA polymerase (0.025 U/mL ThermoFisher Scientific, Waltham, Massachusetts, USA), dNTPS (0.2 mM), primers forward and reverse (0.2 μM) and DreamTaq buffer (1X) containing $MgCl_2$ (2.5 mM). Amplification conditions were: $T_{denaturation\_start}$ =95 °C for 2 s; $T_{denaturation}$ =95 °C for 30 s; $T_{annealing}$=54 °C for 30 s; $T_{elongation}$ = 72 °C for 60 s; number of cycles = 35; $T_{elongation\_final}$ = 72 °C, for 10 s. Amplified fragments were run in 1 % agarose gel and visualised by Biodoc-H Imaging System transilluminator (Somatco, Riyadh, Saudi Arabia) in combination with TS Software.

The amplicons obtained were purified with QIAquick PCR purification Kit (Qiagen, Venlo, Netherlands), following the manufacturer's instruction and quantified by using an UV spectroscopy (BioPhotometer, Eppendorf). Amplified DNA was stored at −20 °C in nuclease free water.

The presence of polymorphisms among clinical strains (EC.3, EC.5, EC.6, SA.1, SA.6, SA.10) amplicons was verified by sequencing (Mix2seq kit, Eurofin, Nantes, France) the *932 bp-mdh* and *689 bp-nuc* genes using the primers mentioned in table S.2.

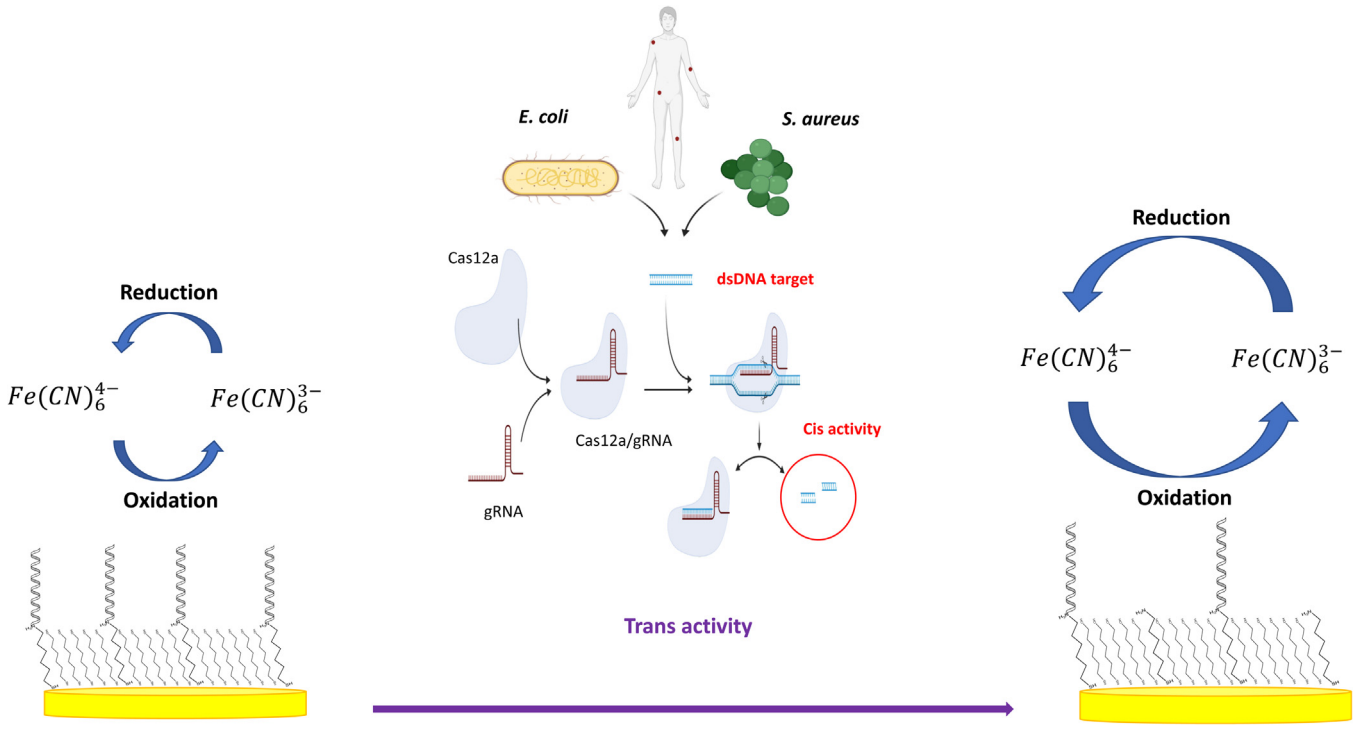

Fig. 1. Schematic representation of the proposed biosensing assay. The ssDNA on the sensor surface hinders the exchange of electrons between the electrode and the solution. Once the Cas12/gRNA system binds and cuts the target DNA, the Cas12 collateral activity is triggered, so that the ssDNA on the electrode surface gets cleaved resulting in a decrease of the charge transfer resistance.

2.3. Evaluation of Cas12a/gRNA activities

2.3.1. RNA guide (gRNA) design

A specific PAM sequence (5' – TTTN– 3') was selected within each selected gene sequence. RNA guides were designed using SnapGene software to have a complementary sequence of 20 nucleotides after the PAM plus a crRNA scaffold (see supplementary table 3). Selected gRNA sequences were compared with an online tool (Eukaryotic Pathogen CRISPR Guide RNA/DNA Design Tool, EuPaGDT). The gRNA sequences were purchased by ThermoFisher scientific (Waltham, Massachussets, USA) in lyophilizate form and resuspended in nuclease free water to a 1 μM solution.

2.3.2. Digestion trial: evaluation of Cas 12a primary activity

Digestion trials were performed on *mdh*- and *nuc*- gene fragments amplified from *E. coli* and *S. aureus* genomic DNAs, respectively. The digestion reactions were performed in 30 μL with a molar ratio LbaCas12a (purchased by New England Biolabs, Ipswich, MA, USA):gRNA:amplified target DNA of 10:10:1, in RNase-free H_2O. The reactions were prepared as follows: 20 μL of nuclease free water, 3 μL of 10X NEB buffer 2.1, 1 μL of 1 μM LbaCas12a (final concentration: 30 nM) and 3 μL of 300 nM gRNA (final concentration: 30 nM). The Cas12a:gRNA complex was allowed to form for 20 min at room temperature, then 3 μL of 30 nM target DNA (final concentration: 3 nM) were added and the solution was incubated at 37 °C for 1 h [22]. Finally, the Cas12 enzyme was inactivated by heating the digestion mixture at 65 °C for 10 min. Results were checked on 2 % agarose gels, using GeneRuler 1 kb DNA (ThermoFisher Scientific, Waltham, Massachussets, USA) as molecular weight marker.

2.3.3. Digestion trial: assessment of Cas12a collateral activity

Single strand DNA probes (ssDNA) were designed by using the NUPAK and mFold Web Server online software tools, and purchased in lyophilizate form from Merck KGaA, Darmstadt, Germany, (see table 3, supporting information). 3 μL of ssDNA solution (16 ng/μL in RNAse free water) were added to the 30 μL LbCas12a/gRNA digestion mixture described in Section 2.3.2 and incubated for 1 h at 37 °C. The Cas12a collateral activity against *E. coli* and *S. aureus* DNA amplicons was checked by 10 % polyacrylamide gel electrophoresis (Invitrogen, ThermoFisher Scientific, Carlsbad, California, USA), performed at 200 V for 40 min in a Cell SureLock Mini-cell chamber (ThermoFisher Scientific, Waltham, Massachusetts, USA). GeneRuler Ultra Low Range was used as DNA Ladder (ThermoScientific, Waltham, Massachussets, USA). The DNA digestion products were thus visualized by staining with SYBR Gold for 30 min (Thermo Fisher Scientific, Waltham, Massachusetts , USA).

2.4. Electrode fabrication

2.4.1. Electrode cleaning and functionalization

A gold disk electrode (⌀ =1 mm, eDAQ, Sydney, Australia) was first polished with slurry alumina (0.3 μm and 0.05 μm for 2 min each), then sonicated in a 3:1 v/v mixture of ethanol and water for 2 min. Next, the electrode was electrochemically cleaned (2 V for 5 s, -0.35 V for 10 s and then 20 scans of cyclic voltammetry (CV) between -0.3 V and 1.55 V with a scan rate of 4 V/s in H_2SO_4 0.5 M, all potentials were referenced vs. Ag/AgCl reference electrode), then rinsed with MilliQ water and dried under a gentle nitrogen flow [23].

The clean electrode was functionalized as follows: a 10 μM SH-$(CH_2)_6$-ssDNA (Biomers; see supplementary information) solution was treated for 1 h with 0.4 mM TCEP (ThermoFischer Scientific, Waltham, Massachusetts, USA) MilliQ water solution. The electrode was incubated with 1 μM SH-$(CH_2)_6$-ssDNA in phosphate buffer (PB; pH 7.0, 0.1 M) for 3 h. After that, the surface was rinsed with MilliQ water and passivated with 2 mM 6-mercaptohexanol (Merck KGaA, Darmstadt, Germany)

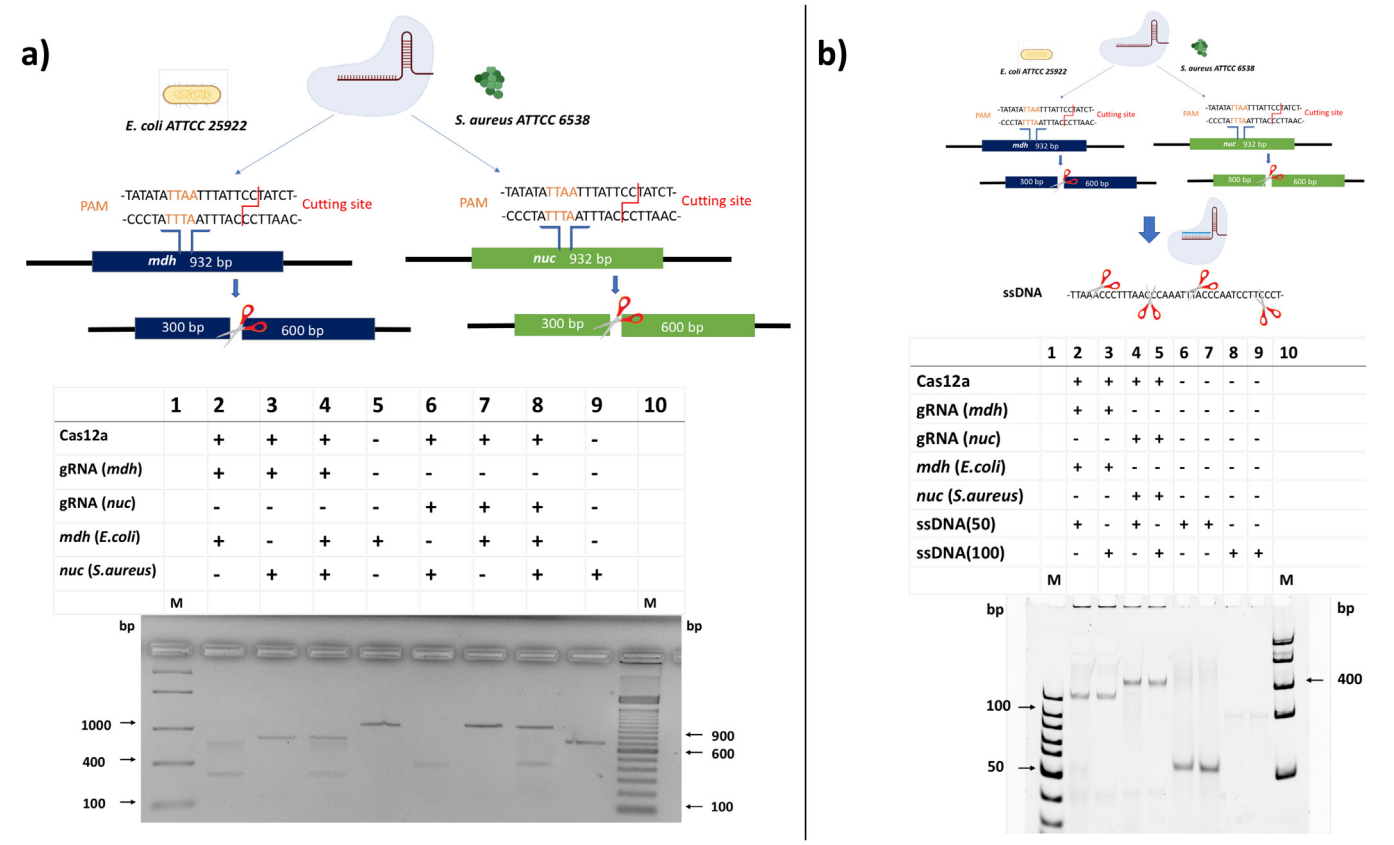

Fig. 2. a) Visualization of the cleavage specificity on a 1 agarose gel. 1) FastRuler middle range DNA 5000-100 bp (ThermoScientific, Waltham, Massachussets, USA); 2) Cas12a + *E. coli* gRNA + *E. coli* target amplicon; 3) Cas12a + *E. coli* gRNA + *S. aureus* target; 4) Cas12a + *E. coli* gRNA + *E. coli* target + *S. aureus* target; 5) *E. coli* Target; 6) Cas12a + *S. aureus* gRNA + *S. aureus* target; 7) Cas12a + *S. aureus* gRNA + *E. coli* target; 8) Cas12a + *S. aureus* gRNA + *S. aureus* target + *E. coli*; 9) *S. aureus* Target; 10) TrackIt DNA ladder 100bp Invitrogen. b) 10 % PAGE in TBE 1 × . The gel shows Cas12a collateral activity upon cleavage of a 50 or 100 nucleotides ssDNA reporter. 1) GeneRuler Ultra Low Range DNA Ladder (ThermoScientific, Waltham, Massachussets, USA); 2) Cas12a + *E. coli* gRNA + *E. coli* target + ssDNA 50 bp; 3) Cas12a + *E. coli* gRNA + *E. coli* target + ssDNA 100 bp; 4) Cas12a + *S. aureus* gRNA + target + *S. aureus* ssDNA 50 bp; 5) Cas12a + *S. aureus* gRNA + *S. aureus* target + ssDNA 100 bp; 6) ssDNA 50 bp room temperature; 7) ssDNA 50 bp 37 °C; 8) ssDNA 100 bp room temperature; 9) ssDNA 100 bp 37 °C; 10) GeneRuler Ultra Low Range DNA Ladder.

MilliQ water solution for 2 h to guarantee the ssDNA organized orientation [24].

CV and EIS were performed in 10 mM $[Fe(CN)_6]^{3-/4-}$ (Merck KGaA, Darmstadt, Germany), phosphate buffer saline (PBS, pH 7 (25 °C), 0.01 M). The electroactive area and DNA density were estimated [25] (S2.2 and S2.2.1).

2.4.2. EIS Cas12a/gRNA investigation

EIS measurements were performed under conditions allowing optimal enzymatic activity in (pH 7.9; 10 mM Tris; 10 mM $MgCl_2$; 50 mM NaCl; at 37 °C), in presence of 10 mM $[Fe(CN)_6]^{3-/4-}$ and with the following parameters (0.22 V DC; 10 mV AC voltage Vs. Ag/AgCl; between $0{,}1-50*10^3$ Hz). Measurements were carried out before and after the Cas12a/gRNA collateral activity action on the electrode modified surface by using a temperature control chamber (ICN 55, ArgoLab). This procedure was also followed for the evaluation of the DNase I (Merck KGaA, Darmstadt, Germany; Lyophilized form) activity.

All electrochemical measurements were performed by the potentiostat/galvanostat/impedance analyser PalmSens4 (PalmSens BV, Houten, Utrecht, Netherlands) in combination with the software PSTrace 5.7.

The impedance spectra were fitted using a Randles equivalent circuit by the PSTrace 5.7. software analyser to obtain charge transfer resistance (R_{ct}) values.

3. Results and discussion

3.1. Assay biosensing principle

The biosensing principle is illustrated in Fig. 1. Upon specific Cas12a/gRNA binding and cleavage of a target dsDNA, ssDNA immobilized on electrode surface are cleaved by the enzyme's trans collateral activity leading to a change in charge transfer resistance, measured by EIS in presence of $[Fe(CN)_6]^{3-/4-}$ redox couple.

3.2. Evaluation of Cas12a/gRNA activities versus E. coli and S. aureus amplified DNAs

A preliminary *in vitro* evaluation of Cas12a/gRNA endonuclease activities was performed on reference strains ATCC25922 and ATCC6538 for *E. coli* and *S. aureus*, respectively. Internal fragment of *mdh* (*E. coli*) and *nuc* (*S. aureus*) genes (Fig. S.1) were amplified, purified and used to assess the ability of the corresponding Cas12a/gRNA complexes to specifically cut the amplicons and to trigger the aspecific collateral activity of the enzyme. Each Cas12a/gRNA complex showed a programmable and specific dsDNA target cleavage activity (Fig. 2a), as well as an indiscriminate collateral activity on ssDNA (Fig. 2b). As shown in Fig. 1a, the ability of the designed *E. coli* and *S. aureus* Cas12a/gRNA complexes to specifically cleave the corresponding dsDNA target was observed only in the presence of the corresponding dsDNA amplicon (Lanes 2,4,6,8). Notably, such cleaving activity was not affected

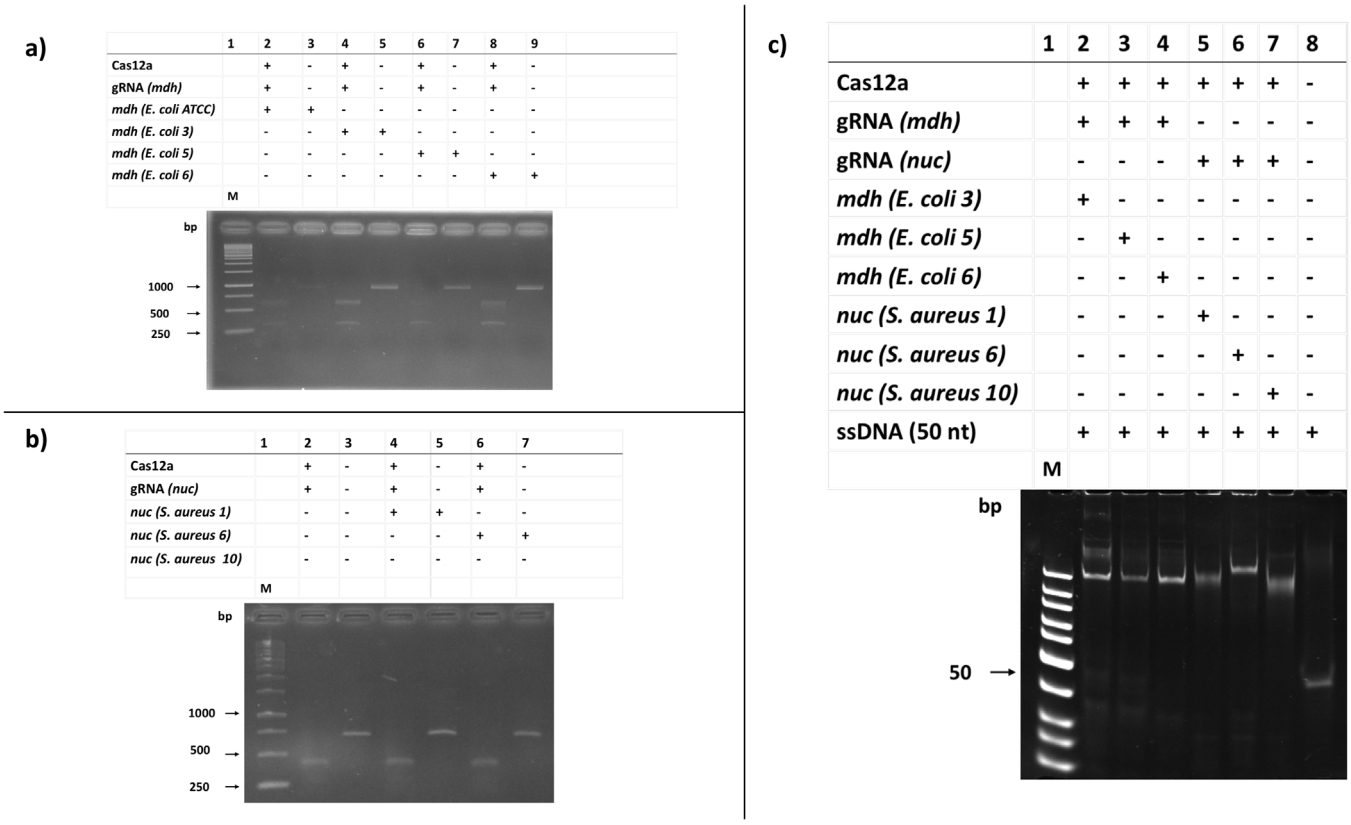

Fig. 3. a) Cas12a/gRNA cleavage of mdh gene fragment amplified from *E. coli* clinical isolates. 1) GeneRuler 1 kb ladder; 2) Cas12a + gRNA + ATCC25922 target; 3) ATCC25922 target; 4) Cas12a + gRNA + EC3 target; 5) EC3 target; 6) Cas12a + gRNA + EC5 target; 7) EC5 target; 8) Cas12a + gRNA + EC6 target; 9) EC6 target. b) Cas12a/gRNA cleavage on *S. aureus* clinical isolates PCR products. 1) GeneRuler 1 kb ladder; 2) Cas12a + gRNA + SA1 target; 3) SA1 target; 4) Cas12a + gRNA + SA6 target; 5) SA6 target; 6) Cas12a + gRNA + SA10 target; 7) SA10 target. c) Collateral activity triggered by clinical isolates PCR products. 1) Ultra Low Range Ladder; 2) Cas12a/gRNA + EC3 target + ssDNA50; 3) Cas12a/gRNA + EC5 target + ssDNA50; 4) Cas12a/gRNA + EC6 target + ssDNA50; 5) Cas12a/gRNA + SA1 target + ssDNA50; 6) Cas12a/gRNA + SA6 target + ssDNA50; 7) Cas12a/gRNA + SA10 target + ssDNA50; 8) ssDNA50.

by the simultaneous presence of non-specific dsDNA obtained from a different bacterial species (Lanes 4 and 8). Conversely, each *E. coli* and *S. aureus* gRNA-complexed enzyme was not able to digest a dsDNA target amplified from a different bacterial species (Lanes 3,7), thus confirming the specificity of the cleaving activity. The endonuclease activity was only exhibited from Cas12a/gRNA complex, while the Cas12a protein alone was not able to cleave the target DNA (Fig. S.2). The programmable activity was only driven by the specific gRNA sequence, and this triggered a multi turnover collateral activity against ssDNA sequences, as previously demonstrated [26].

As depicted in Fig. 2b, ssDNA indiscriminate cleavage activity was observed with 50- (Lanes 6–7) and 100- (Lanes 8–9) nucleotide ssDNA probes, both at 25 °C (Lanes 6,8) and 37 °C (Lanes 7,9). The absence of a band corresponding to the 50- and 100-nucleotide ssDNA in lanes 2,3,4 and 5 was indeed the consequence of collateral activity triggered upon the specific DNA target cleavage by the Cas12a enzyme. The specific activity observed for the designed Cas12/gRNA complexes against the target gene fragments amplified from genomic DNAs of *E. coli* and *S. aureus* reference strains was also evaluated against DNA targets amplified from the genomic DNAs of a panel of *E. coli* and *S. aureus* clinical isolates (Fig. S.3).

This step was important since other studies report that both *E. coli* and *S. aureus* strains responsible for bloodstream infections display genetic heterogeneity, with the presence of several polymorphisms in target genes used in molecular identification studies [27]. These polymorphisms could interfere with the gRNA recognition process, as gRNAs were designed using as template the genome sequence of *E. coli* and *S. aureus* refence strains. Fig. 3 shows specific endonuclease activity of Cas12a/gRNA against a panel of clinical isolates of both bacterial species, obtained from different geographical areas and body sites. Fig. 3 a, b show that the expected cleavage occurred with all *E. coli* (Lanes 2,4,6,8) and *S. aureus* (Lanes 2,4,6) amplified fragments, while Fig. 2c indicates the relative collateral ssDNA activity. Sequencing analysis of the amplified fragment from *E. coli* and *S. aureus* clinical isolates (Fig. S.4) revealed that only one *E. coli* isolate carried a polymorphism in the gRNA target region, but this did not prevent the recognition process and the successive specific cleavage at the desired location. This finding supports the hypothesis that each of the selected gRNA/endonuclease complex is able to selectively and specifically recognize different clinical isolates of *E. coli* and *S. aureus.*

3.3. DNA sensor characterization

The cleaned gold disk electrodes (Fig. S.5) were functionalized with a self-assembled monolayer composed by linear SH-(CH_2)-ssDNA and 6-mercaptohexanol acid (MCH). An optimal length of 20 nucleotide was chosen for the ssDNA probe to obtain a stable and reproducible functionalized layer [24]. In fact, as reported by [17] the 20 nt ssDNA probes had the ideal length to observe the trans-activity of Cas12a/gRNA complex on functionalized electrode. After the functionalization process, the electrodes were characterized electrochemically. Fig. 4a displays results of the chronocoulometric measurements used to estimate the total charge building on the probes upon the interaction of $Ru(NH_3)_6Cl_3$ with the phosphate

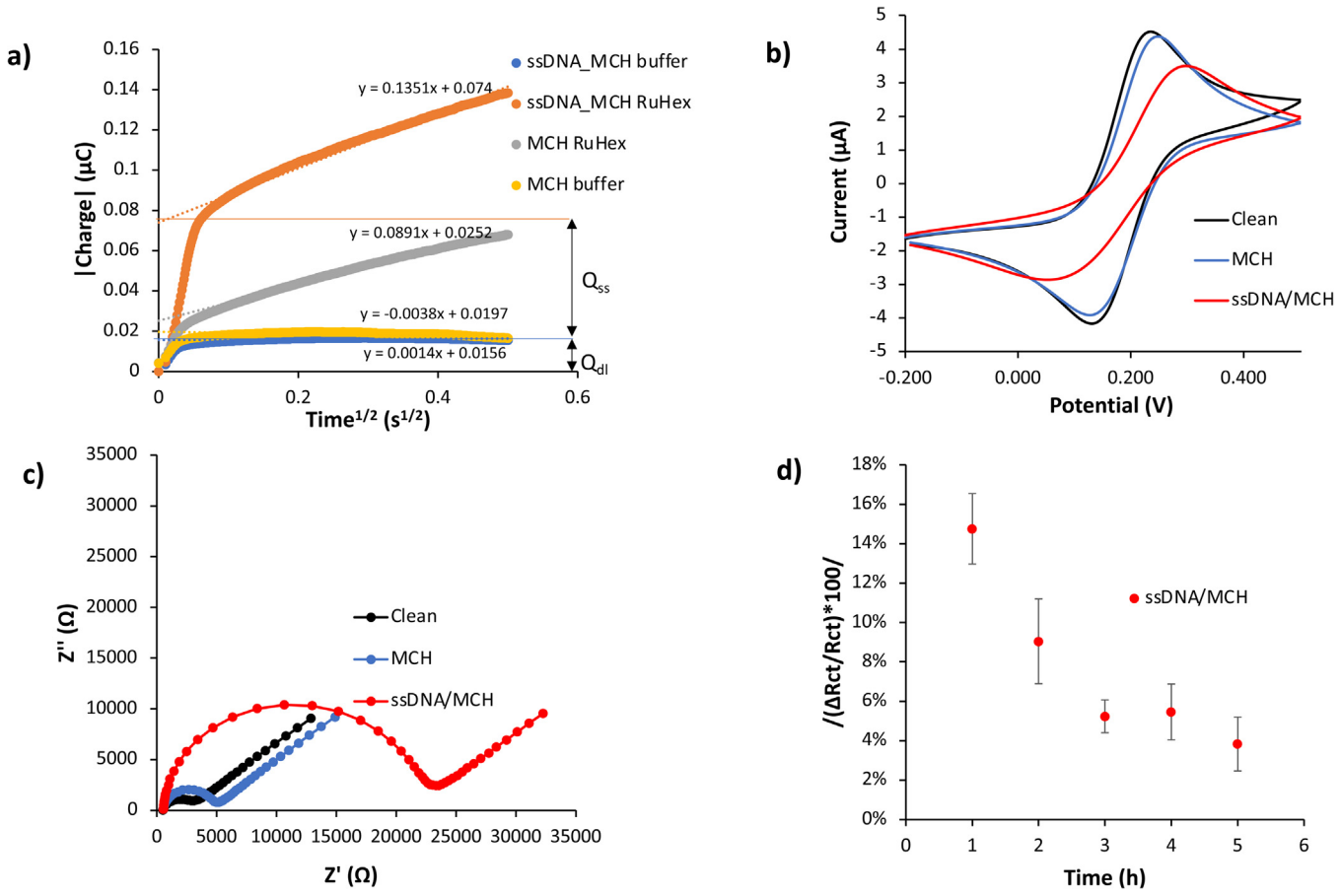

Fig. 4. Comparison of clean and functionalized electrodes: a) Chronocoulometry 10 μ M $Ru(NH3)_6Cl_3$ in Tris 10 mM, pH 7.5, 25 °C b) CV and c) EIS d) Percentage variations of Rct in Tris 10 mM; 10 mM $MgCl_2$; 50 mM NaCl; pH 7.9, 10 mM $[Fe(CN)_6]^{3-/4-}$.

groups of the negatively charged ssDNA, and hence the number of probes and their surface density. Noticeably, a much higher charge gathered on the ssDNA/MCH layer than on the MCH layer, and a value of $(5 \pm 2) \times 10^{12}$ molecules/cm^2 (n = 5) was estimated for the density, which is comparable to what reported in literature for similar functionalization procedures [25]. According to [28], a proper density is utterly important for the nuclease to access the ssDNA probes protruding from the monolayer. Indeed, the endonuclease activity is only possible when the lateral distance (d) between the probes is equal or higher than the enzyme radius. From the calculated density, we estimated a d value of 5 ± 1 nm, so higher than the Cas12a radius (R_{min} = 3.7 nm), that made us choose this functionalization procedure to develop the biosensor (S2.2.1). The use of EIS as electrochemical transduction technique with this kind of dynamic self-assembled monolayer requires a careful control of the measurement conditions [29]. Indeed, EIS measurements involving ssDNA functionalized electrodes are influenced both from the composition of the solution (pH, ionic strength) and external conditions such as temperature [30].To avoid uncontrolled variations of R_{ct}, we decided to use the same solution (pH 7.9; 10 mM Tris; 10 mM $MgCl_2$; 50 mM NaCl; 10 mM $[Fe(CN)_6]^{3-/4-}$) and ambient conditions (37 °C) for all the experiments. The solution was chosen to allow optimal conditions for the endonuclease activity and guarantee a linear ssDNA conformation, whereas temperature was set at the optimal value for the endonuclease activity and carefully controlled. Fig. 4b and c show results of CV and EIS measurements at each functionalization step, i. e. clean, MCH functionalized and ssDNA/MCH functionalized electrode. Short peak to peak distances in cyclic voltammograms and low R_{ct} (obtained from fitting of the Randles equivalent circuit on the EIS spectra) were observed with clean electrodes (ΔCV = 99 ± 1 mV; R_{ct} = 2.1 ± 0.2 kΩ; n = 5), which increased significantly upon functionalization with MCH (ΔCV = 110 ± 3 V; R_{ct} = 5 ± 1 KΩ; n = 5) and ssDNA/MCH (ΔCV = 200 ± 10 mV; R_{ct} = 24 ± 4 kΩ; n = 5). The negative charge of ssDNA and its steric hindrance modified the rate constant of the $[Fe(CN)_6]^{3-/4-}$ redox couple in solution, leading to increased peak to peak distance and R_{ct} value. These increments and results of chronocoulometry confirmed the successful functionalization of the electrode. The dynamism of the ssDNA/MCH functional layer required a stabilization after dipping the electrode in a specific solution [30]. For this reason, we used EIS to measure the R_{ct} hourly for 5 h and verified that 3 h were the optimal time to complete the reorganization process and stabilize the sensitive layer (Fig. 4d). After this time, the biosensor was ready for the addition of the endonuclease enzyme and dsDNA target, and performance of measurements.

3.4. Preliminary measurements with model enzyme

DNase I was chosen as a model enzyme in preliminary EIS measurements for its demonstrated ability to cleave any double or single strand DNA filament [31]. Fig. 5a and b show the Nyquist plot obtained after incubating the sensor for 1 h in active (1.0 mg/mL) and inactive DNase I (1.0 mg/mL of deactivated enzyme at 75 °C for 20 min) solutions, respectively. In the former case, the ssDNA cleavage caused a marked decrease of the overall impedance at every frequency investigated and R_{ct} value due the increased accessibility of the electrode surface from the redox probe [32], which

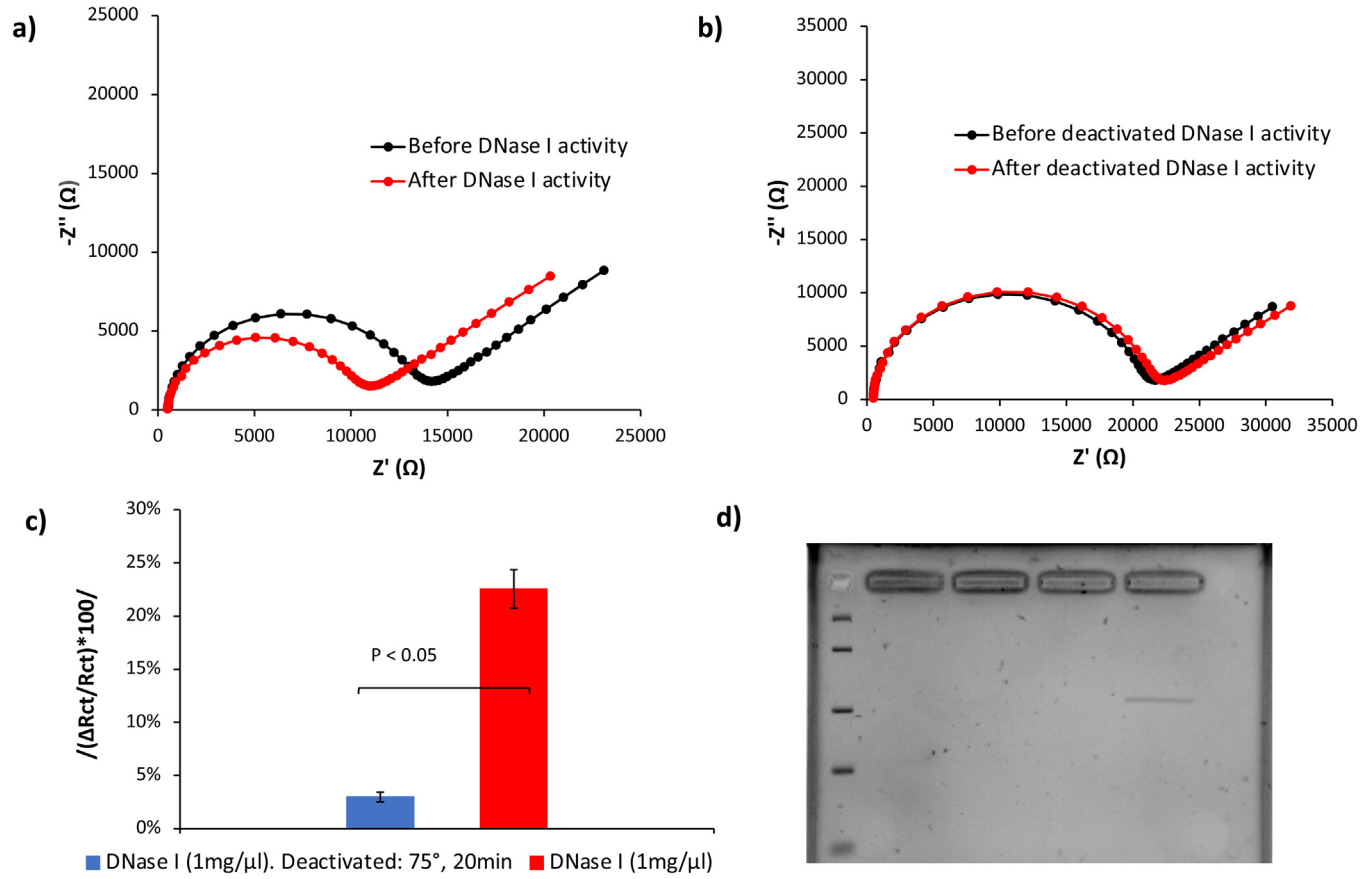

Fig. 5. Early sensor test with DNase I: Nyquist plot of active (a) and deactivated (b) DNase I (1.0 mg/mL); c) Comparison of EIS measurements carried out with active and deactivated DNase I (mean values ± standard deviation, n = 3); d) Gel electrophoresis of the incubation solution: lane 1,2,3 *E. coli* target incubated with DNase I solution, lane 4 pristine *E. coli* target.

was not observed with the inactive enzyme. The impedance variation is better seen in Fig. 5c, which shows that the two sets of measurements are significantly different ($p < 0.05$; $\alpha = 0.05$). To check the activity of DNase I, the *E. coli* DNA target was also incubated in the same solution and the cleavage activity was verified by gel electrophoresis (Fig. 5d). The activity of DNase I was confirmed by the degradation of DNA and the lack of observable bands in lanes 1,2 and 3 (n = 3), whereas lane 4 only contained the control intact DNA target. The experiments with DNase I demonstrated that the enzyme could access and cut the ssDNA on the sensor surface, paving the way to the Cas12a/gRNA biosensor.

3.5. *Cas12a/gRNA biosensing assay performances*

Preliminary tests showed that Bovine Serum Albumin (BSA) and glycerol contained in the commercial buffer by NEB (pH 7.9; 10 mM Tris; 10 mM $MgCl_2$; 50 mM NaCl; 100 µg/µL BSA) and in the Cas12a solution, respectively, interfered with impedance signal, likely by inducing conformational changes on the ssDNA monolayer. The functionalized biosensor was incubated with and without the Cas12a protein both in the commercial buffer and in a laboratory optimized solution without BSA and glycerol (pH 7.9; 10 mM Tris; 10 mM $MgCl_2$; 50 mM NaCl) (Fig. 6a and b). The comparison of Fig. 6a and b shows how the interaction of BSA with the sensitive layer affected the R_{ct} value. This protein assumes, at pH values higher than the isoelectric point (pH 4.7), an unfolded conformation preventing the aggregation [33]. We speculate that this fosters the interaction with the sensitive layer and induces the formation of preferential paths enhancing the exchange of electrons between the electrode and the redox probe. Glycerol in the Cas12a 1 µM stock solution also interfered with the impedance signal (Fig. 6c), so that the 100 µM stock enzymatic solution had to be diluted 100 times to avoid the problem. A concentration of Cas12a/gRNA enzyme complex of 30 nM was chosen as the optimal value for the endonuclease activities [16]. Fig. 6d shows the stable impedance values obtained by incubating the biosensor in the solution containing the Cas12a enzyme under the optimal conditions.

The Cas12a/gRNA activity in this condition was evaluated in parallel by using gel electrophoresis to visualize the cleavage products of PCR amplicons from *E. coli* and *S. aureus* (Fig. S.7). The system was able to recognize and cleave the dsDNA target and the biosensing performances were evaluated against the *E. coli* reference strain. The system was calibrated with different concentrations of dsDNA amplicons in the range 3–18 nM, and signal approached saturation at 9 nM (Fig. 7e and see Table S.4. for EIS parameters assessment). The 3 nM concentration was chosen as the threshold value to distinguish the bacterial amplicon presence. Fig. 7a and b demonstrate the Cas12a/gRNA trans-cleavage activity against 3 nM dsDNA gene target of *E. coli* and *S. aureus*, respectively. Fig. 7c and d show that the EIS signal of active (Cas12a/gRNA in presence of 3 nM of target) and inactive enzyme (Cas12a/gRNA without target) are significantly different ($p < 0.05$; $\alpha = 0.05$), for both *E. coli* and *S. aureus*. The Cas12/gRNA cleavage activity against the incubated dsDNA target in the same solution was also confirmed by gel electrophoresis (Fig. S.8). The same behaviour previously described with DNase I was observed after the Cas12a/gRNA cleavage activity of ssDNA on electrode surface. Therefore, the ability of the Cas12a/gRNA system to access the ssDNA monolayer and exhibit its trans-collateral activity was confirmed on the sensor surface. The use of EIS technique cou-

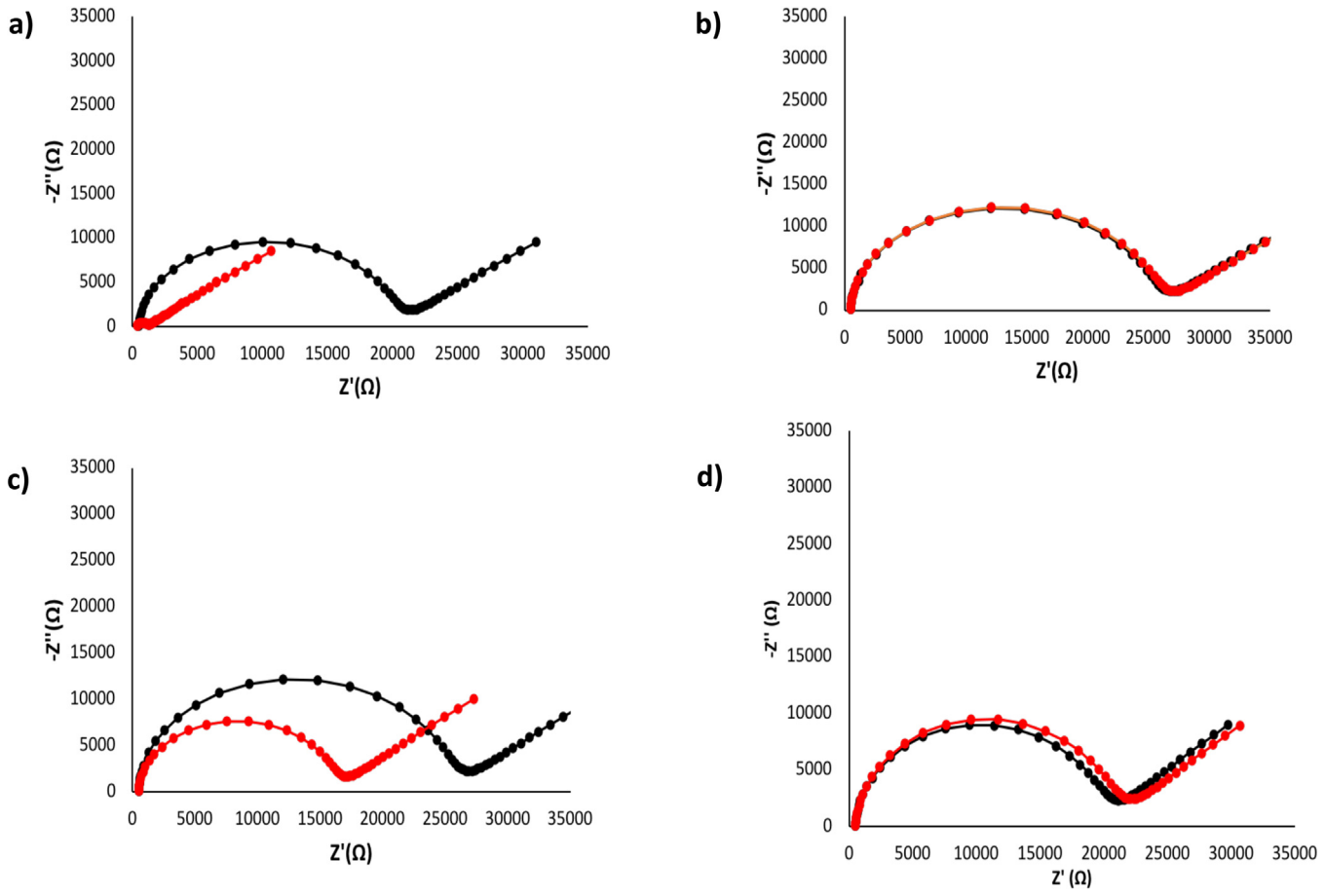

Fig. 6. EIS signal optimization. Black and red curves correspond to EIS measurement before and after incubation process, respectively. a) Nyquist plot following 1 h electrode incubation in (pH 7.9; 10 mM Tris; 10 mM $MgCl_2$; 50 mM NaCl; 100 μg/μL BSA), b) Nyquist plot following 1 h electrode incubation in (pH 7.9;10 mM Tris; 10 mM $MgCl_2$; 50 mM NaCl); c) Nyquist plot in (pH 7.9; 10 mM Tris; 10 mM $MgCl_2$; 50 mM NaCl; 2 % glycerol); d) EIS spectra in (pH 7.9; 10 mM Tris; 10 mM $MgCl_2$; 50 mM NaCl; 0.02 % glycerol).

pled with programmable Cas12a/gRNA system could permit the development of a portable and low-cost biosensing device able to discriminate the presence of bacterial specific genes in solution [20,34]. The programmability of the system allows to perform a portable and reproducible identification of pathogenic bacterial species that could also be easily implemented to tackle the antimicrobial resistance issue, a growing concern in the clinical setting [35]. A major limitation of our assay relies in the response time (around 2 h), since it was not possible to avoid an amplification step from bacterial genomic DNA. However, the implementation of the biosensing assay with an isothermal amplification technique could shorten the time required for the experimental procedure and make it a rapid, specific and portable test for the diagnosis of nosocomial infection. In this case, isothermal amplification (about 20–30 min) and the electrochemical measurement (about 1 h) could reduce the response time to less than 1.3 h, resulting competitive in comparison to traditional laboratory techniques [7]. *E. coli* and *S. aureus* DNA concentrations during BSI infections have been estimated to be about 10^3-10^4 bacterial genome copies/mL [7]. The 3 nM threshold biosensing value used in this study to detect amplified targets represent approximately 5.42×10^{10} gene copies, which could be reached after 15–20 amplification cycles.

4. Conclusions

In this paper, we describe the development of a CRISPR/Cas-based biosensing assay using EIS as electrochemical transduction. The Cas12a/gRNA system combined with a label free ssDNA coated electrode showed a limit of detection of 3 nM for bacterial DNA from *E. coli* and *S. aureus*. Noticeably, the Cas12a/gRNA system selectively and specifically recognized different clinical isolates, demonstrating the biosensor ability to detect different microbial strains and opening the way for its use in diagnostic applications. Currently, the main limitation of this system lies in the response time, which could be reduced by implementing the EIS biosensing assay in a portable, isothermal amplification device avoiding the use of PCR. In fact, despite its outstanding performances, PCR needs costly reagents and a strict temperature control very difficult to obtain in a portable system. Due to the high specificity of the CRISPR/Cas system, we consider that the integration of our system with an isothermal amplification method would not only reduce the analysis time but also the number of false positives commonly affecting isothermal amplification methods. For this purpose, all set up steps of this EIS biosensing assay were presented in detail, to

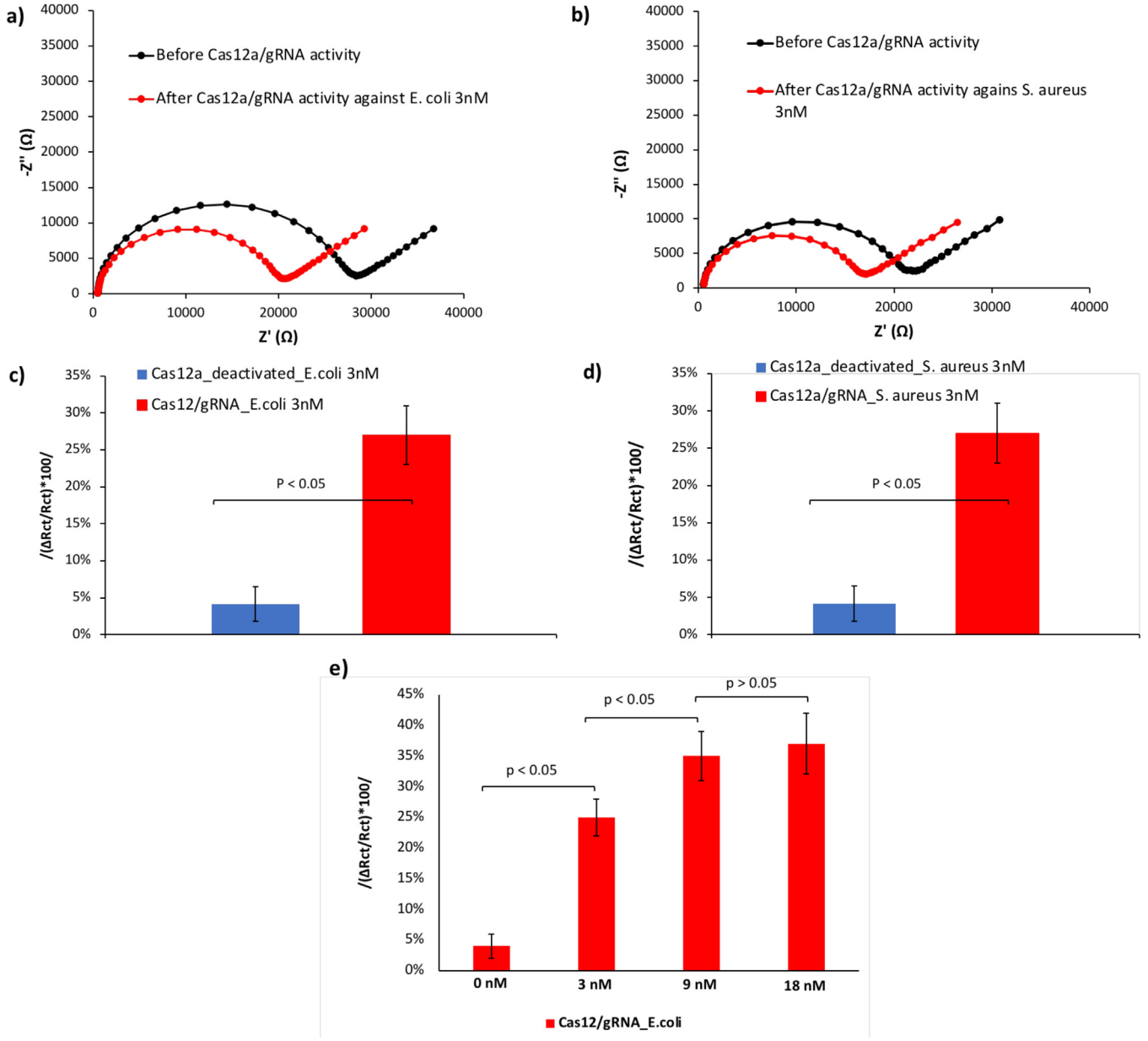

Fig. 7. Results of EIS measurements of CRISPR/Cas activity towards DNA functionalized electrode. a) Nyquist plot with active Cas12/gRNA vs 3 nM *E. coli* and its negative control b) Nyquist plot with active Cas12/gRNA vs 3 nM *S. aureus* and its negative control. c) Bare plot of EIS response with active Cas12/gRNA vs 3 nM of *E. coli* and its negative control d) Bare plot of EIS response with active Cas12/gRNA vs 3 nM of E. coli and its negative control e) EIS Biosensing assay calibration response of Cas12/gRNA Vs *E. coli* target. The plot reports the relative charge transfer resistance depending on *E. coli* target DNA concentration from 3 nM to 18 nM. Data are expressed as mean values ± standard deviation (n = 3).

permit the system implementation and its applicability in further point of care platforms.

CRediT authorship contribution statement

Andrea Bonini: Writing - original draft, Conceptualization, Investigation, Methodology, Formal analysis. **Noemi Poma:** Writing - review & editing, Methodology, Validation. **Federico Vivaldi:** Writing - review & editing, Visualization. **Denise Biagini:** Writing - review & editing, Visualization. **Daria Bottai:** Writing - review & editing. **Arianna Tavanti:** Supervision, Conceptualization, Writing - review & editing. **Fabio Di Francesco:** Supervision, Conceptualization, Writing - review & editing, Funding acquisition.

Declaration of Competing Interest

The authors declare no conflict of interest.

Acknowledgements

The authors gratefully acknowledge Fondazione Pisa is for financial support of the study through the SEMPRE project, and the Center for Instrument Sharing of the University of Pisa (CISUP) for its kind help in the characterization of electrodes.

Appendix A. Supplementary data

Supplementary material related to this article can be found, in the online version, at doi:https://doi.org/10.1016/j.jpba.2021.114268.

References

[1] Z. Saleem, B. Godman, M.A. Hassali, F.K. Hashmi, F. Azhar, I.U. Rehman, Point prevalence surveys of health-care-associated infections: a systematic review, Pathog. Glob. Health 113 (2019) 191–205.

[2] A.J.M. Loonen, P.F.G. Wolffs, C.A. Bruggeman, A.J.C. van den Brule, Developments for improved diagnosis of bacterial bloodstream infections, Eur. J. Clin. Microbiol. Infect. Dis. 33 (2014) 1687–1702.
[3] H. Minasyan, Sepsis and septic shock: pathogenesis and treatment perspectives, J. Crit. Care 40 (2017) 229–242.
[4] R. Markwart, H. Saito, T. Harder, S. Tomczyk, A. Cassini, C. Fleischmann-Struzek, F. Reichert, T. Eckmanns, B. Allegranzi, Epidemiology and burden of sepsis acquired in hospitals and intensive care units: a systematic review and meta-analysis, Intensive Care Med. 46 (2020) 1536–1551.
[5] W. Alhazzani, M.H. Møller, Y.M. Arabi, M. Loeb, M.N. Gong, E. Fan, S. Oczkowski, M.M. Levy, L. Derde, A. Dzierba, B. Du, M. Aboodi, H. Wunsch, M. Cecconi, Y. Koh, D.S. Chertow, K. Maitland, F. Alshamsi, E. Belley-Cote, M. Greco, M. Laundy, J.S. Morgan, J. Kesecioglu, A. McGeer, L. Mermel, M.J. Mammen, P.E. Alexander, A. Arrington, J.E. Centofanti, G. Citerio, B. Baw, Z.A. Memish, N. Hammond, F.G. Hayden, L. Evans, A. Rhodes, Surviving Sepsis Campaign: guidelines on the management of critically ill adults with Coronavirus Disease 2019 (COVID-19), Intensive Care Med. 46 (2020) 854–887.
[6] H. Motbainor, F. Bereded, W. Mulu, Multi-drug resistance of blood stream, urinary tract and surgical site nosocomial infections of Acinetobacter baumannii and Pseudomonas aeruginosa among patients hospitalized at Felegehiwot referral hospital, Northwest Ethiopia: a cross-sectional study, BMC Infect. Dis. 20 (2020) 1–11.
[7] O. Opota, K. Jaton, G. Greub, Microbial diagnosis of bloodstream infection: towards molecular diagnosis directly from blood, Clin. Microbiol. Infect. 21 (2015) 323–331.
[8] S.Y, R.E. Rothman, PCR-based diagnostics for infectious diseases: uses, limitations, and future applications in acute-care settings, Lancet Infect. Dis. 4 (2004) 337–348.
[9] L. Zhang, B. Ding, Q. Chen, Q. Feng, L. Lin, J. Sun, Point-of-care-testing of nucleic acids by microfluidics, TrAC - Trends Anal. Chem. 94 (2017) 106–116.
[10] S. Kumar, S. Tripathy, A. Jyoti, S.G. Singh, Recent advances in biosensors for diagnosis and detection of sepsis: a comprehensive review, Biosens. Bioelectron. 124 (2019) 205–215.
[11] V. Templier, A. Roux, Y. Roupioz, T. Livache, Ligands for label-free detection of whole bacteria on biosensors: a review, TrAC - Trends Anal. Chem. 79 (2016) 71–79.
[12] A. Bonini, N. Poma, F. Vivaldi, A. Kirchhain, P. Salvo, D. Bottai, A. Tavanti, F. Di Francesco, Advances in biosensing: the CRISPR/Cas system as a new powerful tool for the detection of nucleic acids, J. Pharm. Biomed. Anal. 192 (2021), e113645.
[13] J.S. Chen, J.A. Doudna, The chemistry of Cas9 and its CRISPR colleagues, Nat. Rev. Chem. 1 (2017) 1–15.
[14] R. Bruch, M. Johnston, A. Kling, T. Mattmüller, J. Baaske, S. Partel, S. Madlener, W. Weber, G.A. Urban, C. Dincer, CRISPR-powered electrochemical microfluidic multiplexed biosensor for target amplification-free miRNA diagnostics, Biosens. Bioelectron. 177 (2021), e112887.
[15] R. Hajian, S. Balderston, T. Tran, T. deBoer, J. Etienne, M. Sandhu, N.A. Wauford, J.Y. Chung, J. Nokes, M. Athaiya, J. Paredes, R. Peytavi, B. Goldsmith, N. Murthy, I.M. Conboy, K. Aran, Detection of unamplified target genes via CRISPR–Cas9 immobilized on a graphene field-effect transistor, Nat. Biomed. Eng. 3 (2019) 427–437.
[16] Y. Dai, R.A. Somoza, L. Wang, J.F. Welter, Y. Li, A.I. Caplan, C.C. Liu, Inside cover: exploring the trans-cleavage activity of CRISPR-Cas12a (cpf1) for the development of a universal electrochemical biosensor (Angew. Chem. Int. Ed. 48/2019), Angew. Chem. Int. Ed. 58 (2019), e17084.
[17] D. Zhang, Y. Yan, H. Que, T. Yang, X. Cheng, S. Ding, X. Zhang, W. Cheng, CRISPR/Cas12a-mediated interfacial cleaving of hairpin DNA reporter for electrochemical nucleic acid sensing, ACS Sens. 5 (2020) 557–562.
[18] W. Xu, T. Jin, Y. Dai, C.C. Liu, Surpassing the detection limit and accuracy of the electrochemical DNA sensor through the application of CRISPR Cas systems, Biosens. Bioelectron. 155 (2020), e112100.
[19] N. Poma, F. Vivaldi, A. Bonini, P. Salvo, A. Kirchhain, Z. Ates, B. Melai, D. Bottai, A. Tavanti, F. Di Francesco, Microbial biofilm monitoring by electrochemical transduction methods, TrAC Trends Anal. Chem. 134 (2020), e116134.
[20] S. Madison E, J.R. Richards, M. Torres, B. Connor M, J.T. La Belle, Faradaic electrochemical impedance spectroscopy for enhanced analyte detection in diagnostics, Biosens. Bioelectron. 177 (2021), e112949.
[21] Z.O. Uygun, L. Yeniay, F. Giŕgiń Sağın, CRISPR-dCas9 powered impedimetric biosensor for label-free detection of circulating tumor DNAs, Anal. Chim. Acta 1121 (2020) 35–41.
[22] B. Zetsche, J.S. Gootenberg, O.O. Abudayyeh, I.M. Slaymaker, K.S. Makarova, P. Essletzbichler, S.E. Volz, J. Joung, J. Van Der Oost, A. Regev, E.V. Koonin, F. Zhang, Cpf1 is a single RNA-Guided endonuclease of a class 2 CRISPR-cas system, Cell 163 (2015) 759–771.
[23] Y. Xiao, R.Y. Lai, K.W. Plaxco, Preparation of electrode-immobilized, redox-modified oligonucleotides for electrochemical DNA and aptamer-based sensing, Nat. Protoc. 2 (2007) 2875–2880.
[24] A.B. Steel, R.L. Levicky, T.M. Herne, M.J. Tarlov, Immobilization of nucleic acids at solid surfaces: effect of oligonucleotide length on layer assembly, Biophys. J. 79 (2000) 975–981.
[25] A.B. Steel, T.M. Herne, M.J. Tarlov, Electrochemical quantitation of DNA immobilized on gold, Anal. Chem. 70 (1998) 4670–4677.
[26] J.S. Chen, E. Ma, L.B. Harrington, M. Da Costa, X. Tian, J.M. Palefsky, J.A. Doudna, CRISPR-Cas12a target binding unleashes indiscriminate single-stranded DNase activity, Science 360 (2018) 436–439.
[27] H.J. Kim, Q. Choi, G.C. Kwon, S.H. Koo, Molecular epidemiology and virulence factors of methicillin-resistant Staphylococcus aureus isolated from patients with bacteremia, J. Clin. Lab. Anal. 34 (2020), e23077.
[28] M. Deng, M. Li, F. Li, X. Mao, Q. Li, J. Shen, C. Fan, X. Zuo, Programming accessibility of DNA monolayers for degradation-free whole-blood biosensors, ACS Mater. Lett. 1 (2019) 671–676.
[29] J. Kafka, O. Pänke, B. Abendroth, F. Lisdat, A label-free DNA sensor based on impedance spectroscopy, Electrochim. Acta 53 (2008) 7467–7474.
[30] X. Xu, A. Makaraviciute, S. Kumar, C. Wen, M. Sjödin, E. Abdurakhmanov, U.H. Danielson, L. Nyholm, Z. Zhang, Structural changes of mercaptohexanol self-assembled monolayers on gold and their influence on impedimetric aptamer sensors, Anal. Chem. 91 (2019) 14697–14704.
[31] V. Biagiotti, A. Porchetta, S. Desiderati, K.W. Plaxco, G. Palleschi, F. Ricci, Probe accessibility effects on the performance of electrochemical biosensors employing DNA monolayers, Anal. Bioanal. Chem. 402 (2012) 413–421.
[32] Y. Jin, Label-free monitoring of site-specific DNA cleavage by EcoRI endonuclease using cyclic voltammetry and electrochemical impedance, Anal. Chim. Acta 634 (2009) 44–48.
[33] R. Li, Z. Wu, Y. Wangb, L. Ding, Y. Wang, Role of pH-induced structural change in protein aggregation in foam fractionation of bovine serum albumin, Biotechnol. Rep. Amst. (Amst) 9 (2016) 46–52.
[34] E.P. Randviir, C.E. Banks, Electrochemical impedance spectroscopy: an overview of bioanalytical applications, Anal. Methods 5 (2013) 1098–1115.
[35] K. Kiga, X.E. Tan, R. Ibarra-Chávez, S. Watanabe, Y. Aiba, Y. Sato'o, F.Y. Li, T. Sasahara, B. Cui, M. Kawauchi, T. Boonsiri, K. Thitiananpakorn, Y. Taki, A.H. Azam, M. Suzuki, J.R. Penadés, L. Cui, Development of CRISPR-Cas13a-based antimicrobials capable of sequence-specific killing of target bacteria, Nat. Commun. 11 (2020) 1–11.